

**A MATHEMATICAL MODEL for CEREBROVASCULAR
DYNAMICS**

by

Melis Alptekin

B.Sc., Chemical Engineering, Yıldız Technical University, 2007

Submitted to the Institute of Biomedical Engineering

in partial fulfillment of the requirements

for the degree of

Master of Science

in

Biomedical Engineering

Boğaziçi University

2010

ACKNOWLEDGMENTS

Especially, I would like to thank to my advisor Assoc. Prof. Dr Ata AKIN for his precious guidance and opinions. It was a pleasure for me to work with him. In the future, I wish I can find a chance to work with him again.

Thanks to all volunteers participated in my experiments.

I appreciate the help and the guidance of Sinem Burcu ERDOĞAN. I am very grateful to her for sharing me her opinions in every step of this work. She was so kind, this meant the worlds to me.

I would also like to express my gratitudes to Serdar ATEŞ for his assistance with MATLAB. I am very glad he found the time to help me and it was really nice to meet him.

My deepest gratefulness is for Cenk OKYAR who helped me during my fNIRS experiments. Not only he helped me in this study, also he gave me courage and support during the challenges I met. I am very lucky to have found him.

Last but not least, i am very grateful to my mother, grandmother and father for their patience and belief in me during my entire work. Their motivation made me believe, too.

This work is dedicated to my grandfather who passed away in 2000 from Alzheimer's disease.

ABSTRACT

A MATHEMATICAL MODEL for CEREBROVASCULAR DYNAMICS

Human brain goes through a number of physiological changes in daily life. Some of these changes can be observed with optical imaging methods at near infrared light range. The aim of this study is, by using functional near infrared spectroscopy (fNIRS), with a specific experimental protocol, estimating the venous compliance and resistance values of the brain by constructing a three-element Windkessel model and observing oxygenation and blood volume with respect to time. For this purpose, 10 healthy volunteers participated and measurements were taken from their prefrontal cortex during the experiment. When the subjects are in supine position, they were asked to move their heads down to their knees and they stayed in this position for 30 seconds. fNIRS signals were analysed to represent right and left hemisphere. Therefore, in each hemisphere, maximum and minimum points of blood volume showed no significant difference for men and women. (left hemisphere: for V_{min} ; $p=0.12$, for V_{max} ; $p=0.22$; right hemisphere: for V_{min} ; $p=0.073$, for V_{max} ; $p=0.074$). Without taking sex difference into account, V_{min} and V_{max} values of right and left hemisphere are not significantly different (respectively $p=0.22$, $p=0.069$). For compliance values, there is not a meaningful difference between left and right hemisphere. ($p=0.38$). For resistance values between right and left hemisphere, we found a significant difference ($p=0.04$). Therefore, this study implies that there is not a meaningful difference in a young subject group with respect to brain hemodynamics and parameters but only the resistance values. This model may be also used in an elderly or diseased group to observe brain hemodynamics.

Keywords: head-down tilt, fNIRS, Windkessel models

ÖZET

SEREBROVASKÜLER DİNAMİKLER İÇİN BİR MATEMATİKSEL MODEL

İnsan beyni, günlük hayat içinde çevresel uyaranlar karşısında birçok fizyolojik değişime uğramaktadır. Özellikle beyin damarlarındaki bu değişimler, yakın kızıl altı ışık aralığında ışına yapan optik görüntüleme metoduyla incelenebilir. Bu çalışmanın amacı, spesifik bir deney protokolü ile işlevsel yakın kızılaltı spektroskopisi (fNIRS) ile, oksijenlenme ve kan hacmini gözlemleyerek, oluşturulan üç elemanlı Windkessel modeline göre beynin venöz komplians ve direnç değerlerini tahmin etmektir. 10 sağlıklı denegin prefrontal korteksinden ölçümler alınmıştır. Deneklerden, oturur pozisyondayken, kafalarını diz hizasına kadar eğdikten sonra 30 saniye boyunca aynı pozisyonda kalmaları istenmiştir. Bu hareketin sonlanmasıyla birlikte, oksijenlenme ve kan hacmi miktarlarındaki değişim izlenmiştir. fNIRS sinyalleri, beynin sol ve sağ yarımküresini temsil etmek üzere 6'şarlı gruplar halinde analiz edilmiş ve her iki yarımkürede, kan hacminin erkek ve kadınlar açısından maksimum ve minimum noktaları arasında anlamlı bir fark bulunamamıştır (sol yarımküre: V_{min} $p=0.12$, V_{max} $p=0.22$; sağ yarımküre: V_{min} $p=0.073$, V_{max} $p=0.074$). Kadın-erkek farkı gözetmeden sağ ve sol yarımküreler karşılaştırıldığında da V_{min} ve V_{max} değerleri arasında anlamlı bir fark yoktur (sırasıyla $p=0.22$, $p=0.069$). Komplians değerleri için sağ ve sol yarımkürelerde anlamlı bir fark bulunamamıştır ($p=0.38$). Direnç değerleri için ise, sol ve sağ yarımkürede anlamlı bir fark gözlemlenmiştir. ($p=0.04$). Bu anlamlılık değerlerine göre, genç deneklerden oluşan yaş grubunda direnç değerleri dışında beyin hemodinamikleri ve parametreleri göz önüne alındığı zaman, büyük değişimler beklenmemektedir. Bu modelin aynı zamanda yaşlı ve hasta bir grup üzerinde beyin hemodinamiklerini gözlemlemek üzere de kullanılabileceği düşünülmüştür.

Anahtar Sözcükler: Windkessel modelleri, kafa-eğme protokolü, fNIRS

TABLE OF CONTENTS

ACKNOWLEDGMENTS	iii
ABSTRACT	iv
ÖZET	v
LIST OF FIGURES	viii
LIST OF TABLES	x
LIST OF SYMBOLS	xi
LIST OF ABBREVIATIONS	xii
1. INTRODUCTION	1
1.1 Motivation and Objectives	1
1.2 Contribution of the Thesis	2
1.3 Outline of the Thesis	2
2. CEREBROVASCULAR DYNAMICS	3
2.1 Compliance	3
2.1.1 Arterial Compliance	4
2.1.2 Venous Compliance	5
2.1.3 Vascular Compliance	6
2.2 Vascular Resistance	7
2.3 Windkessel Models	7
2.4 Functional Near Infrared Spectroscopy (fNIRS)	10
2.5 Head-Down Tilt Procedure	12
3. METHODS	15
3.1 Subjects	15
3.2 Experimental Design	15
3.2.1 Experimental Protocol	15
3.2.2 fNIRS Measurements	16
3.3 Data Analysis	17
3.4 Mathematical Modeling	18
3.5 Curve Fitting	22
3.6 Statistics	23

4. RESULTS	24
5. DISCUSSION	29
5.1 Limitations of the Study	30
5.2 Future Works	30
6. CONCLUSION	31
REFERENCES	32

LIST OF FIGURES

Figure 2.1	Arterial compliance pressure-volume curve [3]	3
Figure 2.2	Example of an applanation tonometry [3]	5
Figure 2.3	Linearized model of the pressure-volume relationship in the arterial and venous system [4]	6
Figure 2.4	One element model with with one resistor. R_1 represents total peripheral resistance [15]	8
Figure 2.5	Three-element model with two resistors and a capacitor [14]	8
Figure 2.6	(a) variable resistor model (b) Voltage-source/diode model [18]	9
Figure 2.7	The photon path inside the human head: Light source (1) Photo detector (2). [19]	11
Figure 2.8	Hb and HbO ₂ versus time graphic of an fNIRS signal detected from forehead. Red lines represent the markers to distinguish time intervals for observation	12
Figure 2.9	Head-down or head-up tilt table [10]	13
Figure 3.1	Head-down tilt procedure at 5 stages	15
Figure 3.2	A 4-LED probe with 10 photodetectors	17
Figure 3.3	Block diagram of data analysis	18
Figure 3.4	The shape of the wave occurs with pulse generator	18
Figure 3.5	Constructed three-element Windkessel model	19
Figure 3.6	Voltage across capacitance when $C= 0.5$ and $R_v=7.5$	20
Figure 3.7	Voltage across capacitance when $C= 1$ and $R_v= 15$	20
Figure 3.8	Voltage across capacitance when $C= 1$ and $R_v= 3$	21
Figure 3.9	Voltage across capacitance when $C= 2$ and $R_v= 7.5$	21
Figure 3.10	Time versus blood volume of left hemisphere modeling on Matlab environment	22
Figure 3.11	Time versus blood volume of right hemisphere modeling on Matlab environment	23
Figure 4.1	BV, HbO ₂ and HBO for left hemisphere	24
Figure 4.2	BV, HbO ₂ and HB for right hemisphere	24

Figure 4.3 R_v differences between two hemispheres

28

LIST OF TABLES

Table 2.1	Analogy of physiological and electrical components.	9
Table 3.1	Initial values used in Figure 3.6, 3.7, 3.8 and 3.9	19
Table 4.1	V_{max} , V_{min} , R_v and C values of male and female subjects on left hemisphere	25
Table 4.2	p values of parameters for difference between males and females on left hemisphere.	25
Table 4.3	V_{max} , V_{min} , R_v and C values of male and female subjects on right hemisphere.	26
Table 4.4	p values of parameters for difference between males and females on right hemisphere	26
Table 4.5	p values for left and right hemispheres for males and females	26
Table 4.6	All parameters for two hemispheres	27
Table 4.7	p values for two hemispheres	27

LIST OF SYMBOLS

C	compliance
$[\text{HbO}_2]$	oxyhemoglobin
$[\text{Hb}]$	deoxyhemoglobin
R_a	arterial resistance
R_v	venous resistance
R_{v2}	variable resistance
R_{v1}	vascular resistance
V_a	arterial voltage
V_v	venous voltage
V_{min}	minimum blood volume
V_{max}	maximum blood volume
V_{ext}	cuff pressure/external pressure
V_{MCA}	velocity in middle cerebral artery
Z_o	characteristic impedance of the proximal aorta

LIST OF ABBREVIATIONS

AP	arterial pressure
BV	blood volume
CBF	cerebral blood flow
CBR	cerebral blood resistance
CBV	cerebral blood volume
CPP	cerebral perfusion pressure
fMRI	functional magnetic resonance imaging
fNIRS	functional near infrared spectroscopy
HDT	head down tilt
ICP	intracranial pressure
MSP	mean systemic pressure
PCB	printed circuit board
THC	total hemoglobin concentration
TOI	tissue oxygenation index

1. INTRODUCTION

1.1 Motivation and Objectives

Compliance is very important in diseases like arteriosclerosis and stroke. With ageing, the probability of developing compliance related diseases is increasing so early diagnosis of these diseases is very essential to minimize the risk. Several methods have been propose to measure the compliance non-invasively. MR-guided catheterization is one of the most common method. Another non-invasive methods, photoplethysmograph, is used which provides an estimation of cutaneous blood flow by measuring the dynamic attenuation of infrared light by the blood volume present in tissue. The changes in arterial compliance can also be continously measured by trancranial Doppler tonometry to monitor the blood velocity in both middle cerebral arteries (V_{MCA}). Asai showed in 2002 that [1], the studies are successful for brain oxygenation and the amount of hemoglobin recording by fNIRS in humans and rabbits. In a human experiment, 45° head down for 3 minutes at standing position was observed. Results showed that this protocol increases cerebral blood volume. In Kurihara's work [2] in 2003, cerebral oxygenation and tissue oxygenation index [TOI] is recorded by fNIRS probe from 5 healthy men. 90° head up and 6° head down protocols are held in 3 different days. It is reported that in head down, oxyhemoglobin and TOI is decreasing while in head down TOI is constant. These methods are useful but clinicians are in need of a more practical equipment. This is why we performed our study.

The aim of this study is to measure hemodynamic parameters in a young and healthy group with functional near infrared spectroscopy (fNIRS). Another aim of this study is by understanding the relationship between them, to propose a valid, first order and three-element mathematical model. We believe this non-invasive method and proposed model will provide a new approach to estimate the compliance and resistance of the cerebral arteries for elderly group easily and more comfortably.

1.2 Contribution of the Thesis

There are two parts of this study. First part is the experimental part and the other part is associated with model. Main contribution of this thesis is to construct a mathematical model for brain hemodynamics and estimate the parameters related with this dynamics with fNIRS. To achieve this:

1. head-down task is performed and applied to make a pressure gradient to measure the blood volume change (ΔBV) due to a posture change.
2. fitting the data gained from volunteers to model output to obtain the suitable parameters.

We aimed to combine the experimental protocol with the designed model to assess estimation of compliance and resistance for future studies.

1.3 Outline of the Thesis

In Chapter 1, the introduction of the thesis is present. Chapter 2 gives information about some parameters of the brain, different models in literature, functional near-infrared spectroscopy and head-down tilt procedure. Chapter 3, explains the methods we used in the thesis; experiment and the model. It also includes subject enrollment, how we applied the task, data analysis and statistics. In Chapter 4 experimental and model results are given. Discussion of the results, limitations of the study and future works are included in Chapter 5. Concluding remarks are in Chapter 6.

2. CEREBROVASCULAR DYNAMICS

Brain vessels have characteristic mechanical where any impairment may lead to diseases. The resistance of blood flow through vessels, ability of expansion due to the pressure applied to the vessel walls are the common mechanical properties. Before mentioning the models, these properties used in models should be defined in order to have information to make accurate comments of physiology of the brain. Compliance, resistance and Windkessel models are discussed in this chapter.

2.1 Compliance

There are three kind of compliances; arterial compliance, venous and vascular compliance which is the sum of two compliance values. Compliance is defined as the change in volume due to a change in pressure as shown in Equation 2.1. In other words, it is the elasticity value of the vessels. In Figure 2.1, the slope of the pressure-volume curve is shown. [3]-[4].

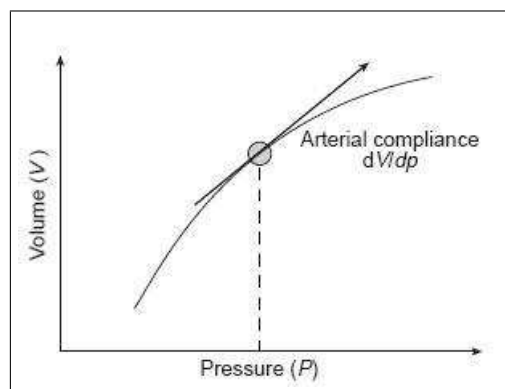


Figure 2.1 Arterial compliance pressure-volume curve [3]

$$C = \Delta V(mL) / \Delta P(mmHg) \quad (2.1)$$

The unit of compliance is usually taken as $\frac{mL}{mmHg}$.

2.1.1 Arterial Compliance

In 1960, Bergel et al held a study to describe the mechanical properties of the arterial wall of a dog with simple incremental modulus of elasticity measurement. This study showed that the arterial wall becomes stiffer as it is extended and compliance is a function of time and not constant during lifetime [5]. In some articles, "compliance" is stated as "stiffness" [6]. Stiffening is the result of increasing systolic pulse pressure, and for decreasing diastolic pressure beyond 40 years of age [6]. Nevertheless, there is an inverse proportion between ageing and arterial compliance in humans. In brief, blood pressure mostly increases with age and when pressure increases in arterial system, arterial compliance decreases [3].

One of the most important aspects of the decreased arterial compliance is hypertension because it reflects an impairment in the the elasticity of the arteries and veins. It is also associated with impaired arterial baroreflex regulation of heart rate [7]. Loss of compliance in arteries means cross-linkage of collagen and reduction in elastic fibres [8].

Invasive and non-invasive methods are used to assess the compliance parameter. In Muthurangu et al's work 17 subjects suspected of pulmonary hypertension or congenital heart disease requiring preoperative assessment underwent MR-guided cardiac catheterization and invasive manometry were used to measure pulmonary arterial pressure [9]. For another example of a non-invasive method; Manwaring suggests that the intracranial pressure (ICP) waveform to the digital artery waveform gives brain compliance. The ICP waveform can be derived from a piezo sensor snugged into the external ear canal and worn as a headset and the digital artery waveform can be derived from a standard pulse oximeter [10]. Several studies have demonstrated that applanation tonometry through the skin provides pressure wave measurements. Non-invasive methods are preferable because it does not require intervention. The procedure is much more comfortable for patients, too. As an example for one of the non-invasive methods, applanation tonometry is widely used. Aortic pressure waveforms were derived from peripheral waveforms and they are recorded by applanation tonometry of the radial

artery [11]. Pencil like probe is placed on the surface and it records the waves from peripheral veins. The position of the transducer on the arteries, the hold-down force and the angle between the transducers and the arterial surface can affect the pressure shape wave, but with practice, clear and repeatable measurements can be obtained [3].

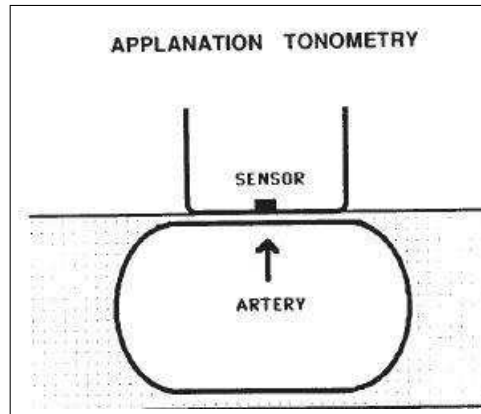


Figure 2.2 Example of an applanation tonometry [3]

Compliance also plays a very important role in diseases and have an increased risk of vascular dementia, stroke, myocardial infarction, arteriosclerosis, autonomic nervous system and other cardiovascular complications [3]-[12]. Today knowing compliance value is significantly lower in people who have one of these diseases than healthy people [7]-[8], models are being constructed to estimate compliance earlier. On the other hand, different treatments are applied to lower the high blood pressure. Anti-hypertensive drugs, physical exercise and hormone replacement therapy helps to reduce blood pressure so to increase arterial compliance [3].

2.1.2 Venous Compliance

As in arterial compliance, the pressure-volume curve slope gives the venous compliance, too, as seen in Figure 2.3 but the curves behaves differently.

The curves in Figure 2.3 are derived from values measured in dogs and are extrapolated to normal humans. The arterial pressure remains constant until the blood volume rises to 0.5 L. This value is called unstressed volume, where the pressure begins to rise. When the volume increases to 0.85 L, arterial pressure comes to 100 mmHg.

In the venous system, unstressed volume and compliance are greater than in arterial system. The unstressed volume is approximately 2.95 L and begins to rise above zero. Figure 2.3 helps to understand the difference between volume-pressure relationship of the arterial and venous system, which is related to anatomical differences between elastic structures in two vascular components. Reduced arterial compliance regulates the systolic function of the heart, reduced venous compliance modulates the changes of diastolic function [4].

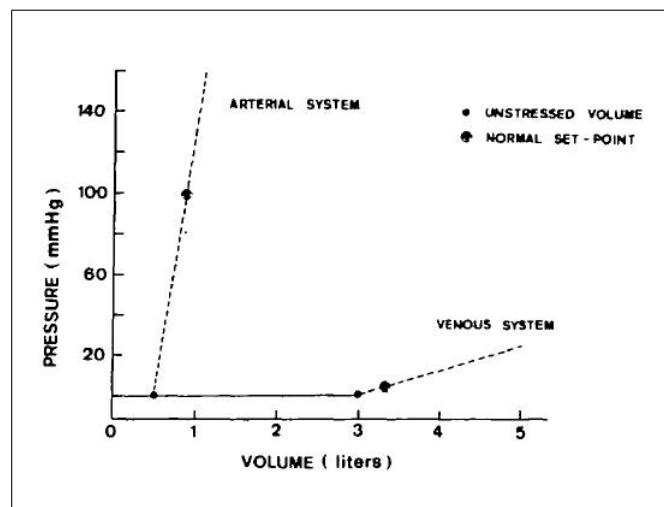


Figure 2.3 Linearized model of the pressure-volume relationship in the arterial and venous system [4]

2.1.3 Vascular Compliance

Mean systemic pressure (MSP) is the intravascular pressure measured when arterial and venous pressures are equal. There is a relation between MSP and blood volume, an index of the elasticity of the system, vascular compliance can be found [4]. Vascular tone refers to the degree of constriction experienced by a blood vessel relative to its maximally dilated state so smooth muscle contraction, which increases vascular tone, reduces vascular compliance; conversely, smooth muscle relaxation increases compliance. Vascular compliance can be determined by non-invasive methods such as (magnetic resonance imaging (MRI) and functional near infrared spectroscopy fNIRS. fNIRS will be discussed in another chapters in details.

2.2 Vascular Resistance

Vascular resistance is a resistance to blood flow through the circulatory system. More the resistance increases, it is harder for blood to flow. Increased cerebrospinal fluid pressure can also lead to high resistance. When cerebral perfusion pressure (CPP) is divided by cerebral blood flow (CBF) it gives cerebral blood resistance (CBR). CBR is influenced by constriction and dilatation of the arterioles in the brain.

2.3 Windkessel Models

Determination the characteristics of the brain hemodynamics is difficult and because of its nonlinear mechanical properties biophysicists and physiologists have been trying to develop simplified representations of this system to describe some of its functional aspects [13]. It is possible to build dynamic models of at least first order [14]. To mimic and represent blood flow and pressure in the arterial system, Windkessel and lumped models are widely used. Some characteristics of the mechanical properties of the whole arterial tree can be derived from the continuous measurements of aortic arterial pressure (AP) and blood flow. These models are derived from electrical circuit analogies where the electrical components represents arterial system components. Advantage of lumped models is; they are easier to solve with simple ordinary differential equations [15].

The Windkessel model was originally generated by Stephen Hales and further developed by Otto Frank in 1899. He used this model to describe blood flow in the heart and systemic arteries. He also used the analogy of an old-fashioned hand-pumped fire engine (in German "Windkessel" pump and this resulted in the development of the original "two-element" Windkessel model). One-element model consists of one resistor but it does not represent the arterial system. The original model includes the arterial compliance and total peripheral resistance [16]. Windkessel model was then expanded to "three-element" model, which has two resistors and a capacitor. When an additional

capacitor is present, it stands for the impedance of the aorta and the large compliance vessels. The three-element Windkessel has become the most widely used and accepted lumped-parameter model of the systemic circulation [17].

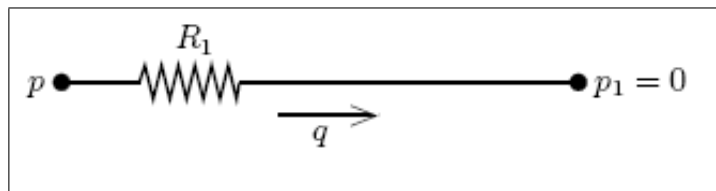


Figure 2.4 One element model with with one resistor. R_1 represents total peripheral resistance [15]

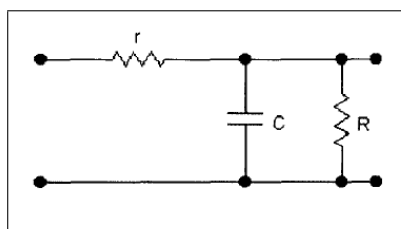


Figure 2.5 Three-element model with two resistors and a capacitor [14]

R , C and r are for the resistance of the microcirculation, the compliance of the large vessels and the characteristic impedance of the proximal aorta, respectively [14].

In Windkessel models, peripheral vessels resistance, arterial and venous resistance are shown R_s , R_a and R_v respectively. In some second or third-order models, the characteristic impedance of the proximal aorta is included and it is nominated as r or Z_o . Meanwhile, the aortic characteristic impedance is generally assumed to be constant over the relatively small pressure range during cardiac cycle [14].

Scientists used the analogy between physiological and electrical components. In Table 2.1 some elements of the lumped models are given.

Table 2.1
Analogy of physiological and electrical components.

Physiological	Electrical
Pressure :	Voltage
Flow :	Current
Viscos drag :	Resistance
Volume :	Charge
Compliance :	Capacitance

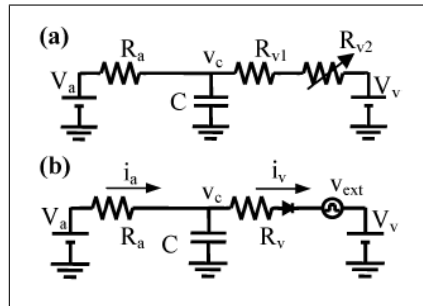


Figure 2.6 (a) variable resistor model (b) Voltage-source/diode model [18]

In Van Ho's study, a mathematical model shown in Figure 2.6 for the hemodynamic response to venous occlusion in human limb has been constructed. The measurements are held with (fNIRS) and and blood volume, blood flow are observed. This model consists of two types: (a) variable resistor model and (b) voltage-source/diode model. In model (a), it has voltage sources V_a and V_v for arterial and venous pressures, respectively. Vascular resistance is modeled by the resistors R_a R_v R_{v1} and R_{v2} and the venous compliance is modeled by C . R_{v2} is the variable resistor that depends on the externally applied pressure. In model (b), v_{ext} represents the influence of cuff pressure. The currents i_a , i_v , R_a , R_v , C also represents the arterial/capillary and venous blood flow, vascular resistances and venous compliance, respectively. The ideal diode implies that the flow never goes in the opposite direction [18]. In this study, we will be modifying this voltage-source/diode model for human brain study.

2.4 Functional Near Infrared Spectroscopy (fNIRS)

It has been reported that neural activity is related to cerebral blood flow (CBF). The close spatial and temporal relationship between neural activity and CBF is known as neurovascular coupling and became the most important concept of neuroimaging techniques that relates the induced cerebrovascular changes to the human brain function. This is also a mechanism which a reduction in local glucose and oxygen stimulates the brain to increase local arteriolar vasodilation, which increases local cerebral blood flow (CBF) and cerebral blood volume (CBV). Oxygenated and deoxygenated hemoglobin ($[HbO_2]$ and $[Hb]$) have different characteristic optical properties in the visible and near-infrared light range so the change in concentration of these molecules can be measured using optical methods non-invasively [19]. The availability to non-invasive monitor cortical tissue was first studied about 30 years ago by F. F. Jöbsis in the study of " Noninvasive infrared monitoring of cerebral and myocardial oxygen sufficiency and circulatory parameter " [20]. Then, in 1993, Chance et al used a simple optical method to cause photon migration from the surface of the head through the skin, skull, and underlying brain tissues to a detector 4 cm distant, also on the surface of the head. Absorption and/or scattering changes of light along the pathway of photon migration are sensitively detected. This simple device is then called fNIRS, a dual wavelength direct-coupled spectrophotometer and can detect changes in the low-frequency components of the light absorption signal from the human brain in response to brain function activity [21]. Functional optical imaging capitalizes on the changing optical properties of the tissues by using light in the near-infrared range (700 - 900 nm) [19]. Calculation of concentration changes of oxy-Hb and deoxy-Hb in blood is based on modified Beer-Lambert Law [22]. When the NIRS measuring site is located over an area in which cerebral blood flow increases during brain activity, a localized increase in $[HbO_2]$ and a decrease in $[Hb]$ could be measured in prefrontal cortex [23]. Regional brain activation is associated with increases in regional cerebral blood flow (rCBF) and the regional cerebral oxygen metabolic rate (rCMRO₂). It is widely accepted that the directions of the changes in oxy-Hb are always the same as those of rCBF and the direction of the changes in deoxy-Hb can be determined by the changes in venous blood oxygenation and volume [24].

The sum of Hb and HbO₂ gives total hemoglobin concentration and so it is equal to blood volume.

$$BV = Hb + HbO_2 \quad (2.2)$$

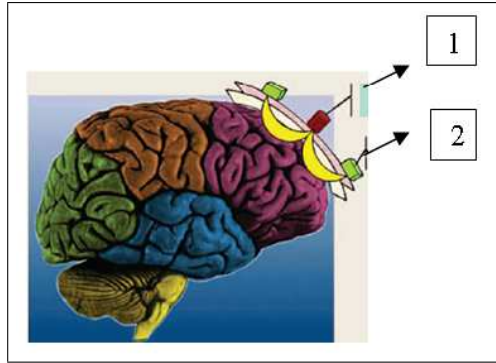


Figure 2.7 The photon path inside the human head: Light source (1) Photo detector (2). [19]

The (fNIRS) apparatus contains a light source that is coupled to the participant's head via either light-emitting diodes (LEDs) or through fiberoptical bundles (the optode) and with a light detector that receives the light after it has interacted with the tissue. Light is scattered after entering the tissue, a photodetector can collect light after it has passed through the tissue. The fNIRS signal becomes sensitive to hemodynamic changes within the top 2-3 mm of the cortex and extends laterally 1 cm to either side, perpendicular to the axis of source-detector spacing [19].

fNIRS can be utilized in neurocognitive processes associated with some neurological (Alzheimer's disease, Parkinson's disease, epilepsy, traumatic brain injury) and psychiatric disorders (schizophrenia, mood disorders, anxiety disorders) [25]. Beside this, it has significant advantages over functional magnetic resonance imaging (fMRI) such as absence of radiation, portable device, user friendliness, no requirement for strict motion restriction and low cost of the procedure [26]. fNIRS can easily be used in infants. NIRS imaging has two major advantages which are it can address issues concerning neurovascular coupling in the human adult and can extend functional imaging approaches to the investigation of the diseased brain [24]-[27]. In contrast, deep

brain structures are hard to measure noninvasively and it is impossible to identify the exact brain areas beneath the light guides [24].

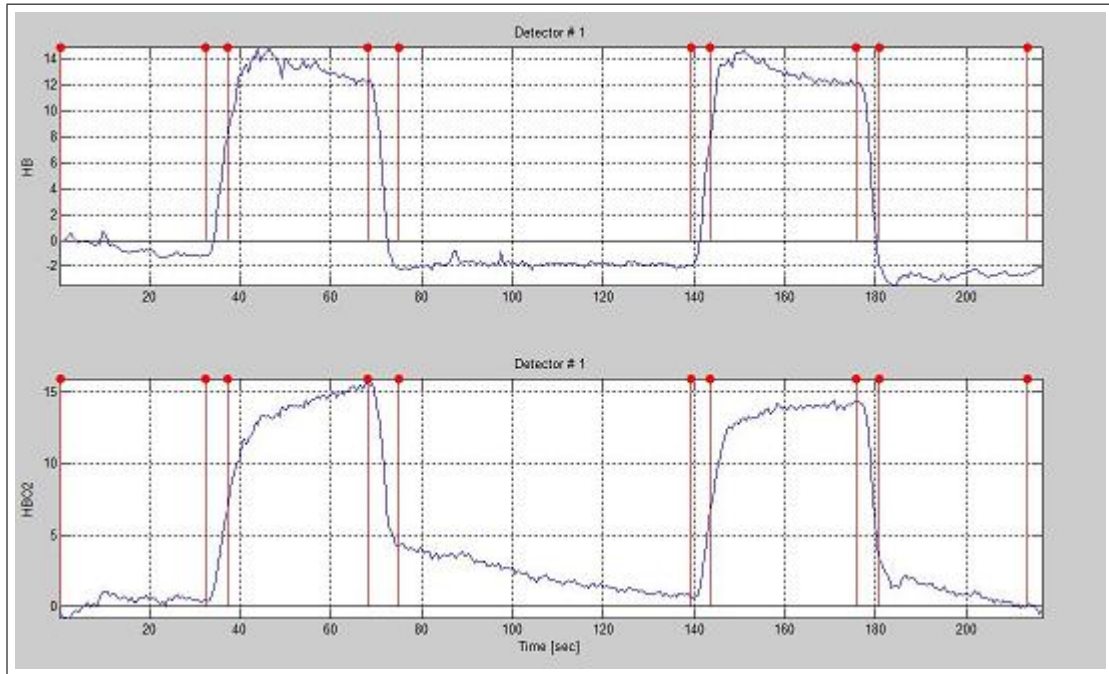


Figure 2.8 Hb and HbO₂ versus time graphic of an fNIRS signal detected from forehead. Red lines represent the markers to distinguish time intervals for observation

2.5 Head-Down Tilt Procedure

Alterations in posture may affect cerebral blood volume and can be used as a therapeutic maneuver to induce or reduce CBV and intracranial pressure [28]. Head-down tilt (HDT) is one of these manoeuvres that produces an increase in intracranial arterial pressure. In fact, HDT causes a blood shift from the limbs towards the chest and the head, so producing increased hydrostatic load of blood [29]. Procedures are usually held by a table tilt which helps patients not to move their heads up or down, but only stay in a constant position fixed onto a table.



Figure 2.9 Head-down or head-up tilt table [10]

However, there are few studies on the various degrees of HDT ($>30^\circ$ angle) on the blood pressure and heart rate on human subjects. For this reason, acute effects of 30° , 60° and 80° HDT were examined with calibrated aneroid sphygmomanometer [30]. The results demonstrated, the 30° head-down showed no significant changes in blood pressure and heart rate. During 60° and 80° HDT, there is a decline in stroke volume [30]. In Asai et al.'s work [1], they studied the effects of head-down tilt from upright to supine position on humans and rabbits by means of transcranial Doppler technique and NIRS [1]. In 12 normal subjects (6 male and 6 female), brain oxygenation (BO_2) and hemoglobin concentration are increased above the baseline. They also examined the effects of 75° head-down versus 45° head-down and suggested that the cerebral blood flow is well tolerated against HDT up to 45° but not to 75° . The constancy of CBF may be because the cross-sectional area of the middle cerebral artery has decreased while the flow velocity increased during HDT [1]. Edlow et al. [31] held an experiment on 60 subjects with (diffuse correlation spectroscopy) DCS /NIRS hybrid optical technique, to find out how healthy aging affects cerebrovascular dynamics at different postures: head-of-bed 30° , supine, standing and supine. In this study, supine-to-standing posture change caused significant declines in regional CBF, THC and HbO_2 , and an increase in Hb, across the age continuum, healthy aging did not alter postural changes in frontal cortical regional CBF and was associated with a smaller magnitude of decline in HbO_2 during supine-to-standing posture change. It is concluded that healthy aging does not alter postural changes in frontal cortical perfusion [31]. Another similar study about the effect of aging on brain oxygenation during changes in position was held by Gatto et al [32]. Oxyhemoglobin and deoxyhemoglobin concentrations were determined from the forehead using NIRS in healthy volunteers. Results were consistent with Edlow's

work. There was a small but significant decrease in HbO_2 and an increase in Hb from supine to sitting position, and this effect was found similar between young and older subjects. Regulation of brain oxygenation during modest decreases in blood pressure did not change in normal aging to 60 years compared to young adults [32].

Up to date, the most frequently technique used to measure the effects of HDT are transcranial Doppler and NIRS. The procedure consists of three steps i) resting position (sitting or upright standing) ii) HDT at different angles for some minutes iii) recovery to supine position. HDT time can change from seconds to hours depending on the procedure. Rabbit experiments can long for hours, but in human experiments it is difficult for human subjects to make them stay at different angles for hours.

3. METHODS

3.1 Subjects

Ten healthy young volunteers (5 male and 5 female) participated in the study. The mean age, height and weight of the participants with standard deviations are; 25 ± 4 , 171 ± 11 cm, 65 ± 14 kg, respectively. All of them were graduate or undergraduate students. Eighty percent of them were not smoking and they have no history of respiratory diseases. None of the them were taking cardiovascular-acting medications. Before they undergo the experiment, procedure and requirements were explained verbally.

3.2 Experimental Design

3.2.1 Experimental Protocol

NIROXCOPE 401 was ready for gathering data to computer and calibrated before each measurements and the probe was placed on the forehead. It is fixed with a bandage to make sure it fully contacts the forehead. Participants were asked not to talk or move in other directions but only perform head-down task so to minimize motion artifacts. The head-down tilt protocol occurs in 5 stages as in Figure 3.2.

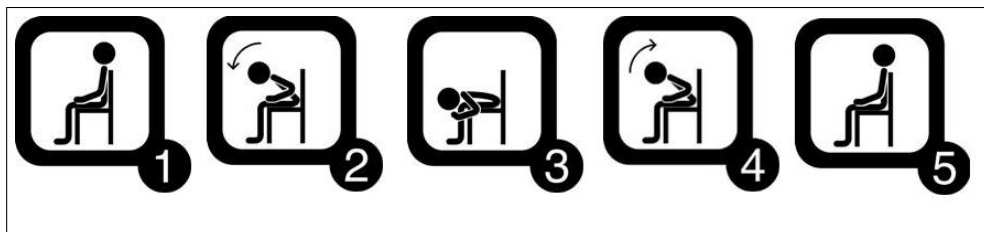


Figure 3.1 Head-down tilt procedure at 5 stages

1. Volunteers were asked to sit straight for 60 seconds.
2. They began to move their head in 5-6 seconds down to their knees approximately to 90°.
3. They kept on staying in head-down position for 30 seconds.
4. They moved their heads back up to supine position in 5-6 seconds.
5. Recovery to supine position and resting for 60 seconds.

All volunteers performed this task without any trouble. This procedure causes blood to flow and to produce a pressure gradient across the head and brain activation can be easily measured by that way. We assumed the pressure change between sitting and head-down position is approximately 5 mmHg.

3.2.2 fNIRS Measurements

To investigate the brain hemodynamics (i.e: changes in HbO₂ and Hb concentrations with respect to time in the cortex), NIROXCOPE 401 has been developed in Boğaziçi University at Neuro-Optical Imaging laboratory and fNIRS measurements are acquired by this device. This non-invasive device is capable of transmitting near-infrared light at two wavelengths (730 and 850 nm), which can penetrate through the scalp and probe the cerebral cortex. This device is composed of:

1. transmitter/receiver circuits which control the LEDs, light sources with the software and LED currents
2. a software to control the device and store the data on the computer for offline analysis
3. a probe consists of detectors and light sources on a flexible printed circuit board
4. a laptop computer (with a DAQ card) to send control signals to the probe.

The probe of the device have 4 light-emitting diodes (LEDs) and 10 detectors. It can sample 16 different channels in the brain simultaneously. Each diode is coupled with its four neighboring sensors, yielding a total of 16 available channels. The raw data is acquired from the probe which is pre-filtered and processed in the data processing unit. The distance between each source and detector is 2.5 cm and probing depth is approximately 2.0 cm from the scalp [22]. Printed circuit board (PCB) is designed to fit the forehead of a human. Sampling frequency of the device is 1.6 Hertz.



Figure 3.2 A 4-LED probe with 10 photodetectors

3.3 Data Analysis

We performed the analysis of data on MATLAB R2006a environment. Measurements of concentration changes of oxyhemoglobin and deoxyhemoglobin in blood are based on modified Beer-Lambert Law. Rather than taking into account of these changes, blood volume change is considered. Maximum point of blood oxygenation (V_{max}) and minimum point after head-down (V_{min}) ended are recorded. The raw data acquired from the probe where pre-filtered and processed in the data processing unit. The data were then sent to the DAQ card to be digitized and read by the computer. The computer either saves the data for off-line analysis or analyzes the received data in real-time. Signals are also sent from the computer through the DAQ to the probe in order to control the photodiodes and sensors. To compare the brain functions laterally, we take the mean of the first 8 channels as left hemisphere and the other 8 channels as right hemisphere. Poor contact of the probe to the forehead can effect the photodiode data. After, data smoothing, we fit the data to the constructed model for estimation.

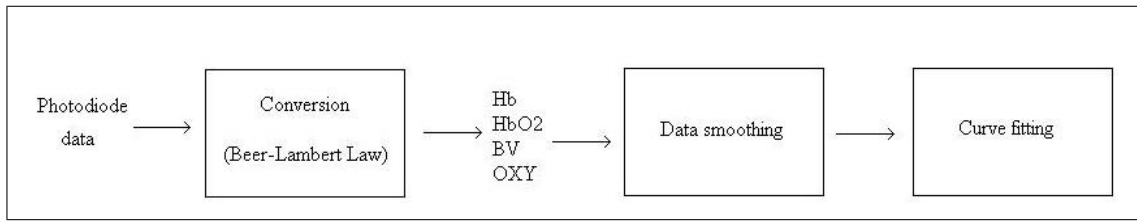


Figure 3.3 Block diagram of data analysis

3.4 Mathematical Modeling

In order to fit the experiment to a model, three-element Windkessel model is constructed on Simulink. Two resistances are used as arterial and venous resistance of the brain and the vascular compliance is represented with a capacitor. The idea of using the pulse generator was inspired from Fantini's work. In Figure 3.4, the shape of the wave output of pulse generator can be shown. The graph is drawn on PSpice environment. One of the most important thing in this work is, the voltage across the

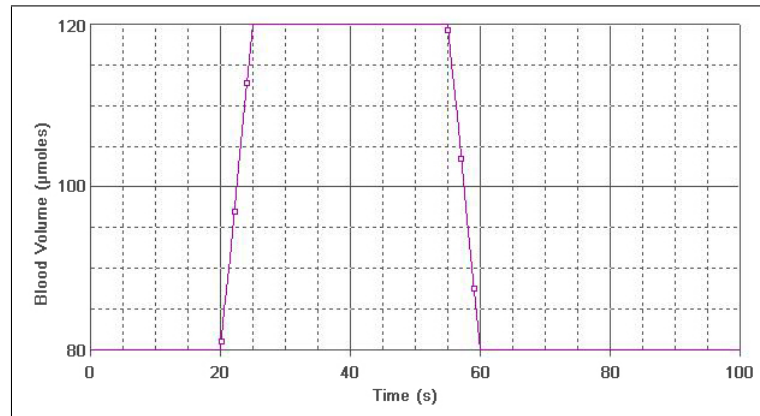


Figure 3.4 The shape of the wave occurs with pulse generator

capacitor is measured and this is thought to be the analogy of the total blood volume of the brain. The model constructed in Simulink is shown in Figure 3.5. The generator simulates the head-down tilt and connected in series with the arterial resistance (R_a) as shown in Figure 3.4. Capacitor (C) is connected in parallel with venous resistance. Arterial pressure and venous pressure are 80 mmHg and 5 mmHg, respectively at each fitting constantly.

To understand how the signal changes when the capacitance and resistance values change, examples are given above. V_{ext} , V_a and V_v are kept constant.

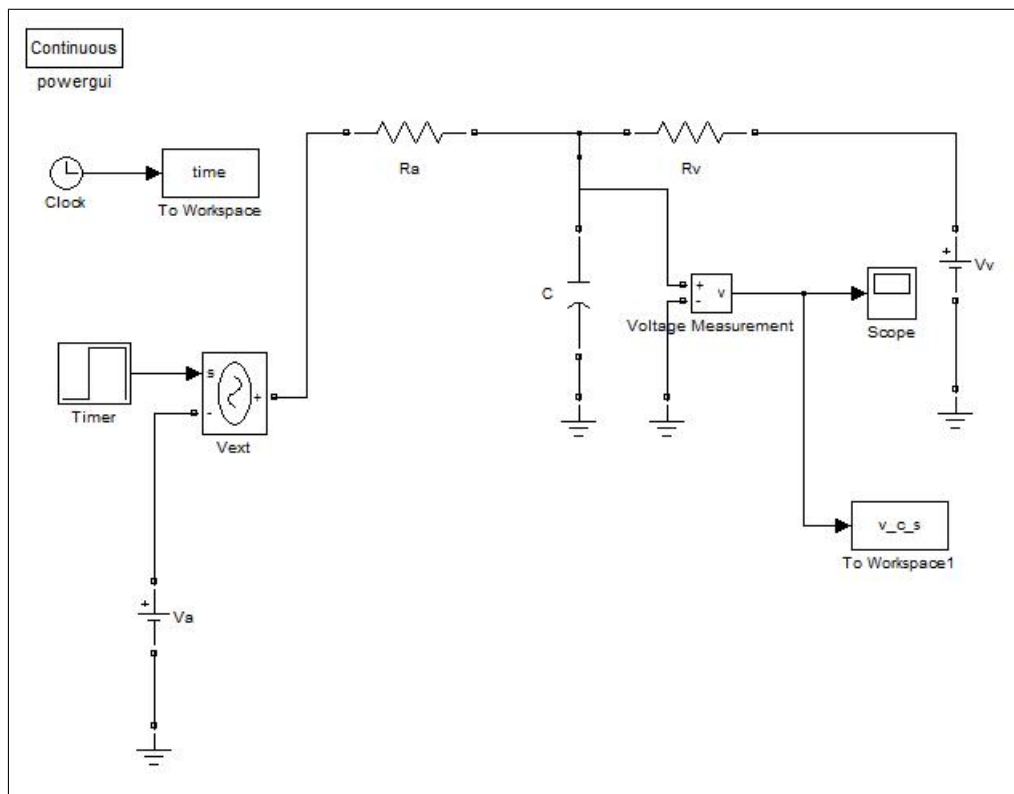


Figure 3.5 Constructed three-element Windkessel model

In Table 3.1, initial values used in Figure 3.6, 3.7, 3.8 and 3.9 are shown..

Table 3.1
Initial values used in Figure 3.6, 3.7, 3.8 and 3.9

R_v (mmHg / (ml/s))	C (ml/mmHg)
7.5	0.5
15	1
3	2

In Figure 3.6, 3.7, 3.8 and 3.9, voltage across the capacitor are shown.

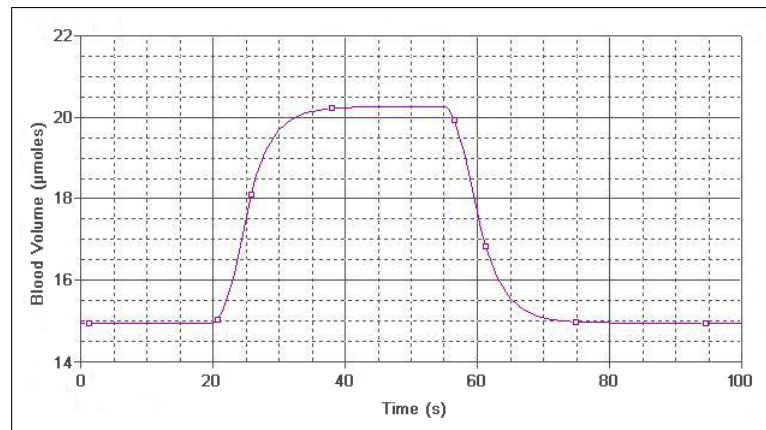


Figure 3.6 Voltage across capacitance when $C = 0.5$ and $R_v = 7.5$

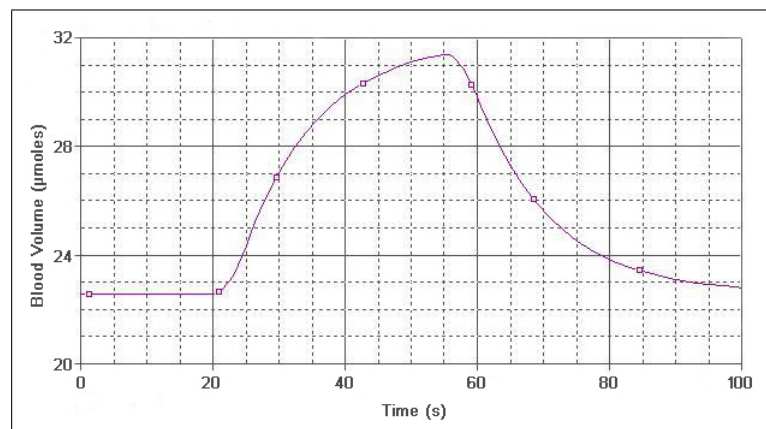


Figure 3.7 Voltage across capacitance when $C = 1$ and $R_v = 15$

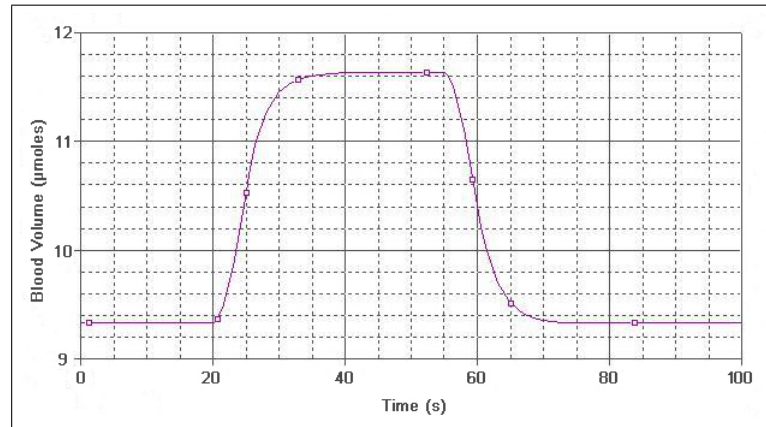


Figure 3.8 Voltage across capacitance when $C = 1$ and $R_v = 3$

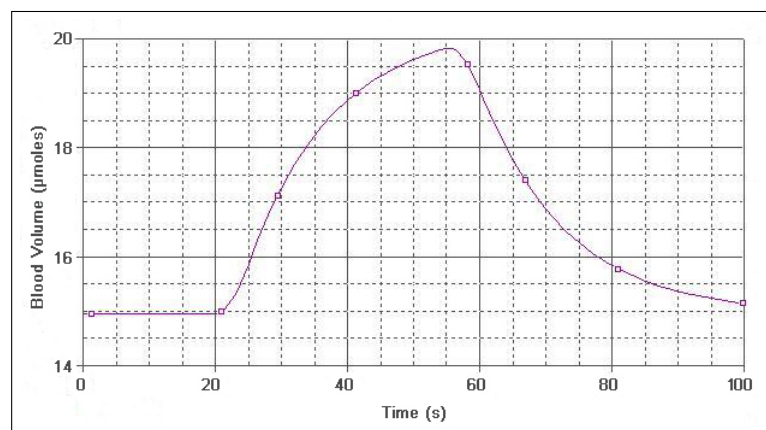


Figure 3.9 Voltage across capacitance when $C = 2$ and $R_v = 7.5$

3.5 Curve Fitting

To execute the fitting, firstly a series of Matlab codes are run to come up with a blood volume signal. After that, model on Simulink is run and fNIRS signal observed from the experiment is constructed on the same axes. They are normalised to make them start for model fitting, error values, which are the square of the difference between data and model parameters, are set at $E < 0.1$. Parameter estimation is done manually, changing the R_v and C values until the error is under 0.1.

In Figure 3.10 and 3.11 modelling of one subject's left and right hemispheres are shown.

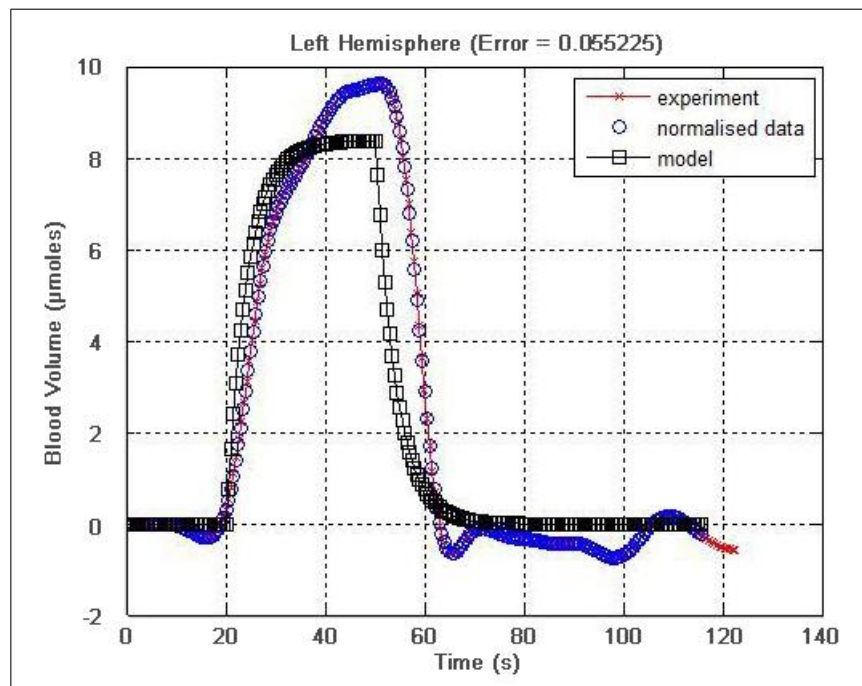


Figure 3.10 Time versus blood volume of left hemisphere modeling on Matlab environment

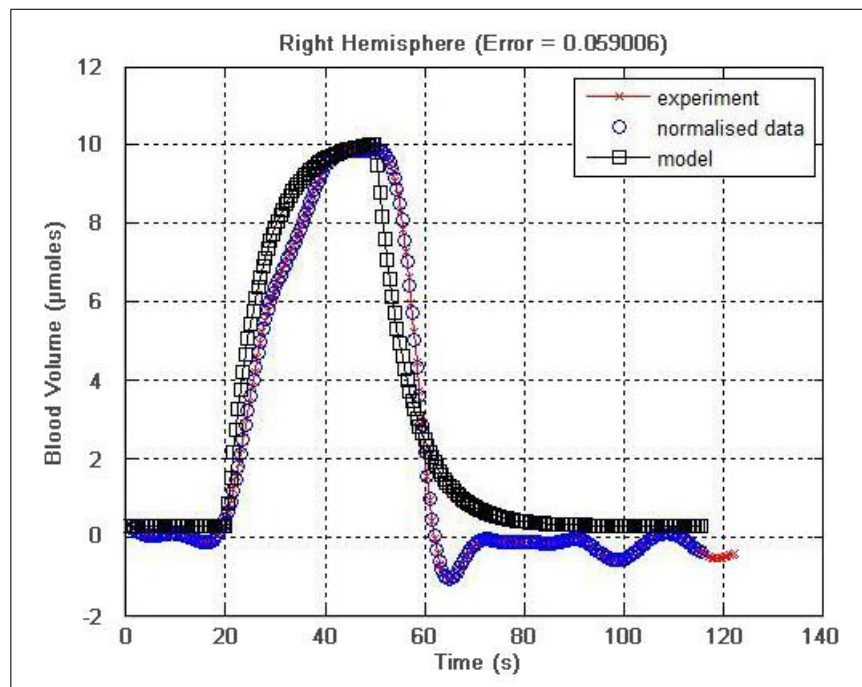


Figure 3.11 Time versus blood volume of right hemisphere modeling on Matlab environment

3.6 Statistics

Paired t-test was used on ten subjects. Statistical significance was set at $P < 0.05$ for all comparisons. Values are means \pm SD. Significant difference of (V_{max}), (V_{min}), resistance and compliance between left and right hemisphere and between sexes are calculated.

4. RESULTS

By head-down tilt procedure, it is observed that in all subject, BV, HbO₂ and HB are increased as shown in Figure 4.1 and 4.2.

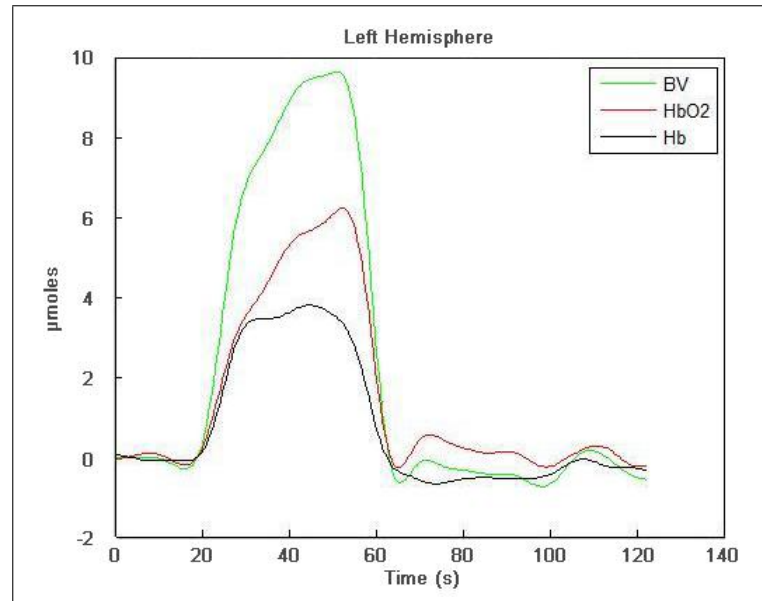


Figure 4.1 BV, HbO₂ and HBO for left hemisphere

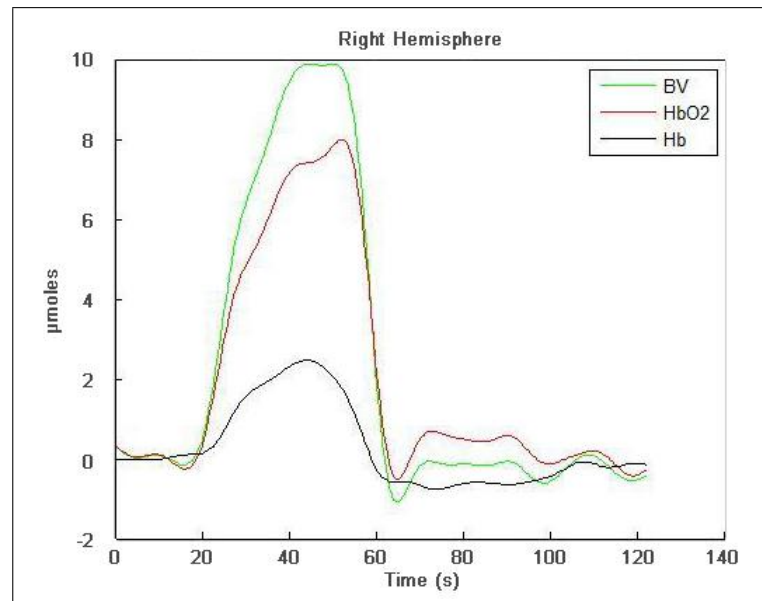


Figure 4.2 BV, HbO₂ and HB for right hemisphere

In all subjects, fNIRS experiments are done, curve fitting for two hemispheres are carried out. For each subject, V_{max} , V_{min} , R_v and C values are calculated. In table 4.1 and 4.2, p value for male and female on each hemisphere can also be seen. All V, R_v and C values are written in terms of micromoles, mmHg /(ml/s) and ml/mmHg respectively.

Table 4.1
 V_{max} , V_{min} , R_v and C values of male and female subjects on left hemisphere

	V_{max}		V_{min}		R_v		C	
	M	F	M	F	M	F	M	F
Subject 1	14.914	9.63	-1.154	-0.6492	28	13	0.11	0.4
Subject 2	6.542	11.278	-1.146	-1.707	9	16	0.4	0.15
Subject 3	23.312	13.301	1.371	-0.278	51	24	0.11	0.42
Subject 4	19.014	12.649	-1.345	0.618	39	22	0.1	0.24
Subject 5	12.939	12.141	2.906	-0.523	21	19	0.19	0.19
Mean	15.344	11.7998	0.126	-0.508	29.600	18.800	0.182	0.280
STD	6.332	1.421	1.917	0.833	16.180	4.438	0.127	0.123

Table 4.2
p values of parameters for difference between males and females on left hemisphere.

	V_{max}	V_{min}	R_v	C
p	0.218	0.258	0.094	0.125

The p value for each hemisphere shows there is not a meaningful difference between male and female subjects in terms of V_{max} , V_{min} , R_v and C. Same results are present for right hemisphere in Table 4.3.

Table 4.3
 V_{max} , V_{min} , R_v and C values of male and female subjects on right hemisphere.

	V_{max}		V_{min}		R_v		C	
	M	F	M	F	M	F	M	F
Subject 1	35.798	10.758	0.983	-1.017	152	16	0.02	0.55
Subject 2	6.081	8.874	-1.155	-2.116	8	11	0.4	0.3
Subject 3	23.691	25.228	2.037	0.803	55	82	0.1	0.2
Subject 4	22.337	15.464	-0.042	0.482	47	25	0.078	0.21
Subject 5	30.439	11.188	4.695	-0.702	138	19	0.079	0.18
Mean	23.669	14.302	1.304	-0.510	80.000	30.600	0.135	0.288
STD	11.226	6.566	2.236	1.181	62.141	29.177	0.151	0.154

In table 4.4, p values of parameters for difference between males and females on right hemisphere are given.

Table 4.4
p values of parameters for difference between males and females on right hemisphere

	V_{max}	V_{min}	R_v	C
p	0.073	0.074	0.073	0.076

To compare if there is a statistical and meaningful difference in right and left hemisphere for each parameter in males and females, p values are calculated as shown in Table 4.5.

Table 4.5
p values for left and right hemispheres for males and females

	V_{max}		V_{min}		R_v		C	
	M	F	M	F	M	F	M	F
p	0.093	0.215	0.199	0.499	0.059	0.199	0.306	0.465

For the next step, we combined the subjects and examine the left and right hemisphere difference without taking sex difference into account.

Table 4.6
All parameters for two hemispheres

	LEFT H.				RIGHT H.			
	V_{max}	V_{min}	R_v	C	V_{max}	V_{min}	R_v	C
Subject 1	14.914	-1.154	28	0.11	35.798	0.983	152	0.02
Subject 2	6.542	-1.146	9	0.4	6.081	-1.155	8	0.4
Subject 3	23.312	1.371	51	0.11	23.691	2.037	55	0.1
Subject 4	19.014	-1.345	39	0.1	22.337	-0.042	47	0.078
Subject 5	12.939	2.906	21	0.19	30.439	4.695	138	0.079
Subject 6	9.63	-0.649	13	0.4	10.758	-1.017	16	0.55
Subject 7	11.278	-1.707	16	0.15	8.874	-2.116	11	0.3
Subject 8	13.301	-0.278	24	0.42	25.228	0.803	82	0.2
Subject 9	12.649	0.618	22	0.24	15.464	0.482	25	0.21
Subject 10	12.141	-0.523	19	0.19	11.188	-0.702	19	0.18
Mean	13.572	-0.191	24.2	0.231	18.986	0.397	55.3	0.2117
STD	4.713	1.433	12.550	0.129	9.977	1.938	52.654	0.165

For all parameters except R_v , there is again not a statistical difference between right and left hemisphere.

p values for two hemispheres are given in Table 4.7.

Table 4.7
p values for two hemispheres

	V_{max}	V_{min}	R_v	C
p	0.069	0.225	0.043	0.387

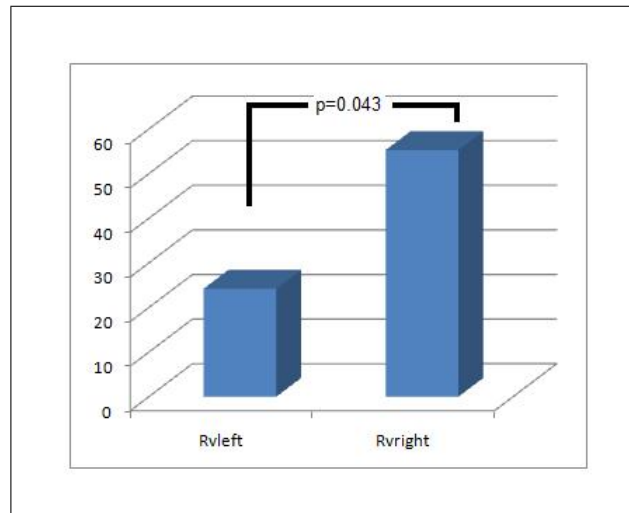


Figure 4.3 R_v differences between two hemispheres

R_v showed statistical difference between left and right hemisphere ($p < 0.05$). This states that, in a young and healthy group, resistance values are different between two hemispheres of the brain.

5. DISCUSSION

Blood volume, compliance and resistance of vascular system are key points to observe how the brain vessels behaves in neurodegenerative diseases. Our model of brain hemodynamic response to head down tilt provides a tool to extract information about these parameters.

In Asai's and Kurihara's work [1]-[2], it is suggested that head down tilt increases cerebral blood flow and our findings are consistent with these studies. Lovell et al [28] found a correlation between changes in CBV and the degree of table tilt in awake subjects. They stated that CBV decreased with 18° head-up tilt and increased with 18° head-down tilt ($P < 0.0001$, $r = -0.924$). Our tilt was approximately 90° and in Vijayalakshmi's study [30], the increase in diastolic pressure was directly proportional to angle of tilt and statistically significant for 60° and 80° ($P < 0.01$ for both), too.

Our study showed, there is a significant increase in BV, Hb0₂ and HB with 90° head down tilt. In male volunteers, all parameters were higher although not significant than female volunteers thus increasing the overall mean of the values. To our knowledge, there is not a study investigating the right and left hemisphere parameter differences. Hemispheric asymmetry is discussed in some papers but they are about the verbal and mental activities, not physical activation. Our aim was to study two hemispheric differences. As we expected in a specific young and healthy group, V_{max} , V_{min} and C are identical. R_v values are not identical between right and left hemisphere and this information carries weight for further works.

This similarity across the parameters can be due to age spectrum. In younger and healthy group, it's more unlikely to have a cerebrovascular disease. If we had chosen older people for the experiment, we might have observed the differences and the results could be different than young and healthy group. This hypothesis is highly important.

5.1 Limitations of the Study

As stated before, in a young group we expected to see no difference in all the parameters between hemispheres; so the difference in resistance values between right and left hemisphere made us think on some experimental problems. It was hard to take the measurements in a quite and isolated room and due to protocol difficulty, volunteers were slowly moving their heads down to their knees. The rate of down and up movement of the head in every person was different and this can effect the magnitude of the fNIRS signal. The use of tilt table could eliminate these kind of rate problems.

Age, height, weight, smoking habits and medication use were asked to volunteers but we did not take into account blood pressure and pulses of the people. We could use pulse oxymeter and phymomanometer. Smoking habit effects the vessel oxygenation so it would be highly related with our work. Hand ability affects the hemisphere side -left or right- people are using so questions about hand ability may be also related with our experiment.

5.2 Future Works

Our first aim for future works is to perform the same experiment in elderly people especially hypertensive group and compare the results with the young group. Thereby, we expect to see the difference in parameters between two groups and this makes our model more practical. Genetic factors can be included, so people, whose one of the family members developed arteriosclerosis, may be examined. Experiments can be held in more people with a more comfortable procedure like using head down tilt table.

6. CONCLUSION

Brain hemodynamics are worth to be observed and take make interest day after day. Many of diseases related with cerebrovascular abnormalities can be detected by methods non- or invasively. In our work, we proved that a non-invasive method, fNIRS, is useful and reliable to find the relationship between brain hemispheres and vascular components. Consistent with the literature, our results showed when the pressure increases in brain vessels, blood volume also increases. Only significant difference in right and left hemisphere is between resistance values and this result is argumantative and needs more deeper study. Set up model will be helpful for future works to early diagnose the diseases and this work can be the first step.

REFERENCES

1. Asai, Y., S. Inonue, K. T. Y. Shiraishi, and Y. Kawai, "Effects of head-down tilt on cerebral blood flow in humans and rabbits," *Proceedings of Life In Space for Life on Earth, 8th European Symposium on Life Sciences Research in Space, 23rd Annual International Gravitational Physiology Meeting*, pp. 195–196, June 2002.
2. Kurihara, K., A. Kikukawa, and A. Kobayashi, "Cerebral oxygenation monitor during head-up and -down tilt using near-infrared spatially resolved spectroscopy," *Clin Physiol Funct Imaging*, Vol. 23(4), pp. 177–81, July 2003.
3. Rajkumar, C., S. Bonapace, and C. Bulpitt, "Arterial compliance in older people," *Reviews in Clinical Gerontology*, Vol. 10, pp. 43–54, 2000.
4. Safar, M., and G. M. London, "Arterial and venous compliance in sustained essential hypertension," *Hypertension*, Vol. 10, pp. 133–139, 1987.
5. Bergel, D. H., "The static elastic properties of the arterial wall," *J Physiol*, Vol. 156, pp. 445–457, 1961.
6. O'Rourke, M. F., J. A. Staessen, C. Vlachopoulos, D. Duprez, and G. E. Plante, "Clinical applications of arterial stiffness definitions and reference values," *AJH*, Vol. 15, pp. 426–444, 2002.
7. Cook, J., A. E. DeVan, J. L. Schleifer, M. M. Anton, M. Y. Cortez-Cooper, and H. Tanaka, "Arterial compliance of rowers: implications for combined aerobic and strength training on arterial elasticity," *Am J Physiol Heart Circ Physiol*, Vol. 290, pp. 1596–1600, 2006.
8. Dhoat, S., K. Au, and C. J. B. C. Rajkumar, "Vascular compliance is reduced in vascular dementia and not in alzheimer's disease," *Age and Ageing*, pp. 1–7, August 2008.
9. Muthurangu, V., D. Atkinson, M. Sermesant, M. E. Miquel, S. Hegde, R. Johnson, R. Andriantsimiavona, A. M. Taylor, E. Baker, R. Tulloh, D. Hill, and R. S. Razavi, "Measurement of total pulmonary arterial compliance using invasive pressure monitoring and mr flow quantification during mr-guided cardiac catheterization," *Am J Physiol Heart Circ Physiol*, Vol. 289, pp. 1301–1306, 2005.
10. Manwaring, P., D. Wichern, M. Manwaring, J. Manwaring, and K. Manwaring, "A signal analysis algorithm for determining brain compliance non-invasively," *Proceedings of the 26th Annual International Conference of the IEEE EMBS*, pp. 353–356, September 2004.
11. Papaioannou, T. G., K. S. Stamatelopoulos, E. Gialafos, C. Vlachopoulos, E. Karatzis, J. Nanas, and J. Lekakis, "Monitoring of arterial stiffness indices by applanation tonometry and pulse wave analysis: Reproducibility at low blood pressure," *J Clin Monit 2004*, Vol. 18, pp. 137–144, 2004.
12. Altunkan, S., K. Oztas, and B. Seref, "Arterial stiffness index as a screening test for cardiovascular risk: A comparative study between coronary artery calcification determined by electron beam tomography and arterial stiffness index determined by a vitalvision device in asymptomatic subjects," *European Journal of Internal Medicine*, Vol. 16, pp. 580–584, August 2005.
13. Molino, P., C. Cerutti, C. Julien, G. Cuisinaud, M.-P. Gustin, and C. Paultre, "Beat-to-beat estimation of windkessel model parameters in conscious rats," *Am J Physiol Heart Circ Physiol*, Vol. 274, pp. 171–177, 1998.

14. Cappello, A., Y. Hong, H. Fang, and G. He, "Identification of the three-element windkessel model incorporating a pressure-dependent compliance," *Annals of Biomedical Engineering*, Vol. 23, pp. 164–177, 1995.
15. Olufsen, M., and A. Nadim, "On deriving lumped models for blood flow and pressure in the systemic arteries," *Mathematical Biosciences and Engineering*, Vol. 1, pp. 61–80, June 2004.
16. Berger, D. S., T. Cui, and j K-J Li, "Stroke volume estimation incorporating a nonlinear arterial system compliance model," *IEEE*, pp. 137–138, 1989.
17. Stergiopoulos, N., E. B. Westernof, and N. Westerhof, "Total arterial inertance as the fourth element of the windkessel model," *Mathematical Biosciences and Engineering*, Vol. 276, pp. 81–88, 1999.
18. Vo, T. V., P. E. Hammer, M. L. Hoimes, S. Nadgir, and S. Fantini, "Mathematical model for the hemodynamic response to venous occlusion measured with near-infrared spectroscopy in the human forearm," *IEEE Transactions on Biomedical Engineering*, Vol. 54, pp. 573–584, 2007.
19. Izzetoglu, M., S. C. Bunce, K. Izzetoglu, B. Onaral, and A. K. Pourrezaei, "Functional brain imaging using near-infrared technology," *Engineering in Medicine and Biology Magazine IEEE*, Vol. 26, pp. 38–46, 2007.
20. Jöbsis, F. F., "Noninvasive, infrared monitoring of cerebral and myocardial oxygen sufficiency and circulatory parameters," *Science*, Vol. 198, pp. 1264–1267, 1997.
21. Chance, B., Z. Zhuand, C. Unah, C. Alter, and L. Lipton, "Cognition-activated low-frequency modulation of light absorption in human brain," *Proc. Natl. Acad. Sci. USA, Journal of Neuroscience Methods*, Vol. 90, pp. 3770–3774, April 1993.
22. Çiftçi, K., B. Sankur, Y. Kahya, and A. Akın, "Constraining the general linear model for sensible hemodynamic response function waveforms," *Med Biol Eng Comput*, Vol. 8, pp. 779–787, August 2008.
23. Villringer, A., and B. Chance, "Non-invasive optical spectroscopy and imaging of brain function," *Trends in Neurosciences*, Vol. 20, pp. 435–442, 1997.
24. Hoshi, Y., "Functional near-infrared optical ?maging: Utility and limitations in human brain mapping," *Psychophysiology*, Vol. 40, pp. 511–520, 2003.
25. Irani, F., S. M. Platek, S. Bunce, A. C. Ruocco, and D. Chute, "Functional near infrared spectroscopy (fnirs): An emerging neuroimaging technology with important applications for the study of brain disorders," *The Clinical Neuropsychologist*, Vol. 21(1), pp. 9–37, 2006.
26. Çiftçi, K., B. Sankur, Y. P. Kahya, and A. Akın, "Multilevel statistical inference from functional near-infrared spectroscopy data during stroop interference," *IEEE Transactions On Biomedical Engineering*, Vol. 55, pp. 2212–2220, September 2008.
27. Obrig, H., and A. Villringer, "Review article beyond the visible: Imaging the human brain with light," *Journal of Cerebral Blood Flow and Metabolism*, Vol. 23, pp. 1–18, 2003.
28. Lovell, A. T., A. C. Marshall, C. E. Elwell, M. Smith, and J. C. Goldstone, "Changes in cerebral blood volume with changes in position in awake and anesthetized subjects," *Neurosurgical Anesthesia*, Vol. 90, pp. 372–376, 2000.

29. Bosonea, D., V. Ozturk, S. Roatta, A. Cavallinia, P. Tosia, and G. Micielia, "Cerebral haemodynamic response to acute intracranial hypertension induced by head-down tilt," *Functional Neurology 2004*; : 31-35, Vol. 19(1), pp. 31–35, January 2004.
30. Vijayalakshmi, P., and Madanmohan, "Acute effect of 30°, 60° and 80° head-down tilt on blood pressure in young and healthy human subjects," *Indian J Physiol Pharmacol*, Vol. 50(1), pp. 28–32, 2006.
31. Edlow, B. L., M. N. Kim, T. Durduran, C. Zhou, M. E. Putt, A. G. Yodh, J. H. Greenberg, and J. A. Detre, "The effects of healthy aging on cerebral hemodynamic responses to posture change," *Physiol. Meas.*, Vol. 31, pp. 477–495, 2010.
32. Gattoa, R., W. Hoffman, C. Paisansathan, W. Mantulin, E. Gratton, and F. T. Charbela, "Effect of age on brain oxygenation regulation during changes in position," *Journal of Neuroscience Methods*, Vol. 164(2), pp. 308–311, 2007.